



UNIVERSITY of
BRADFORD

Library

The University of Bradford Institutional Repository

<http://bradscholars.brad.ac.uk>

This work is made available online in accordance with publisher policies. Please refer to the repository record for this item and our Policy Document available from the repository home page for further information.

To see the final version of this work please visit the publisher's website. Access to the published online version may require a subscription.

Link to publisher's version: <http://dx.doi.org/10.1016/j.neucom.2016.07.050>

Citation: Tehlah N, Kaewpradit P and Mujtaba IM (2016) Artificial neural network based modelling and optimization of refined palm oil process. *Neurocomputing*. 216: 489-501.

Copyright statement: © 2016 Elsevier B.V. Reproduced in accordance with the publisher's self-archiving policy. This manuscript version is made available under the [CC-BY-NC-ND 4.0 license](https://creativecommons.org/licenses/by-nc-nd/4.0/).



Artificial Neural Network based Modelling and Optimization of Refined Palm Oil Process

N. Tehlah^a, P. Kaewpradit^a, I.M. Mujtaba^{b,*}

^aDepartment of Chemical Engineering, Prince of Songkla University, Songkhla 90112 THAILAND

^bSchool of Engineering, University of Bradford, West Yorkshire BD7 1DP, UK

*Corresponding author. E-mail address: I.M.Mujtaba@bradford.ac.uk (I.M. Mujtaba)

Abstract

The content and concentration of beta-carotene, tocopherol and free fatty acid is one of the important parameters that affect the quality of edible oil. In simulation based studies for refined palm oil process, three variables are usually used as input parameters which are feed flow rate (F), column temperature (T) and pressure (P). These parameters influence the output concentration of beta-carotene, tocopherol and free fatty acid. In this work, we develop 2 different ANN models; the first ANN model based on 3 inputs (F, T, P) and the second model based on 2 inputs (T and P). Artificial neural network (ANN) models are set up to describe the simulation. Feed forward back propagation neural networks are designed using different architecture in MATLAB toolbox. The effects of numbers for neurons and layers are examined. The correlation coefficient for this study is greater than 0.99; it is in good agreement during training and testing the models. Moreover, it is found that ANN can model the process accurately, and is able to predict the model outputs very close to those predicted by ASPEN HYSYS simulator for refined palm oil process. Optimization of the refined palm oil process is performed using ANN based model to maximize the concentration of beta-carotene and tocopherol at residue and free fatty acid at distillate.

Keywords: Artificial Neural network; Refined palm oil process, Falling film molecular distillation; Modelling; Optimization

1. Introduction

Molecular distillation (MD) is a special separation technique [1], and it is widely used in various process such as in pharmaceutical, waste water treatment, food and biological processes [2]. MD operates under vacuum pressure and lower temperature than conventional process, which can prevent decomposition of materials and enhance the quality of product [3, 4]. Moreover, the MD is normally applied for thermally sensitive materials. Three parameters are important which add value to the palm oil and these are tocopherol and beta-

carotene in the bottom stream and contaminant of free fatty acid in the distillate stream. In conventional deodorization of palm oil process, the high temperature operation not only eliminates the free fatty acid from oil but also destroy some of the phytonutrients such as beta-carotene and tocopherol due to their thermal sensitive nature. However, the deodorization of palm oil by MD can overcome the problem. The purpose of this work is to obtain the optimum process parameters in order to recovery high concentration of beta-carotene and tocopherol at residue and free fatty acid at the distillate stream. In previous studies [5-8] the operating variables that affect to quality of oil in molecular distillation are feed flow rate, column temperature, pressure, rolling speed and etc. However, only feed flow rate, pressure and temperature affect the quality of oil in falling film molecular distillation. Moreover, other inputs such as condenser temperature and ambient temperature insignificantly affect to the quality of the oil.

In the absence of a real palm oil MD process, the input-output data for the process (required for developing NN based model) is generated via ASPEN HYSYS simulator. The development of MD in ASPEN HYSYS follows similar procedure of literature work where an MD model for palm oil process was developed using ASPEN PLUS (one flash vessel) and validated the results with DISMOL [9]. In their study binary equimolar mixture of Dibutyl phthalate (DBP) and Dibutyl sebacate (DBS) were fed at 50 kg/hr and 0.133 Pa. Temperature was manipulated to accomplish identical distillation mass ratio (0.2120) with DISMOL. The operating temperature for DISMOL and ASPEN PLUS to achieve the same distillate mass ratio were reported to be 369 K and 336 K [9] respectively and with ASPEN HYSYS[10] it was found to be 335.66 K which is close to that obtained by ASPEN PLUS. The results from DISMOL, ASPEN PLUS and ASPEN HYSYS are shown in (Fig.1).

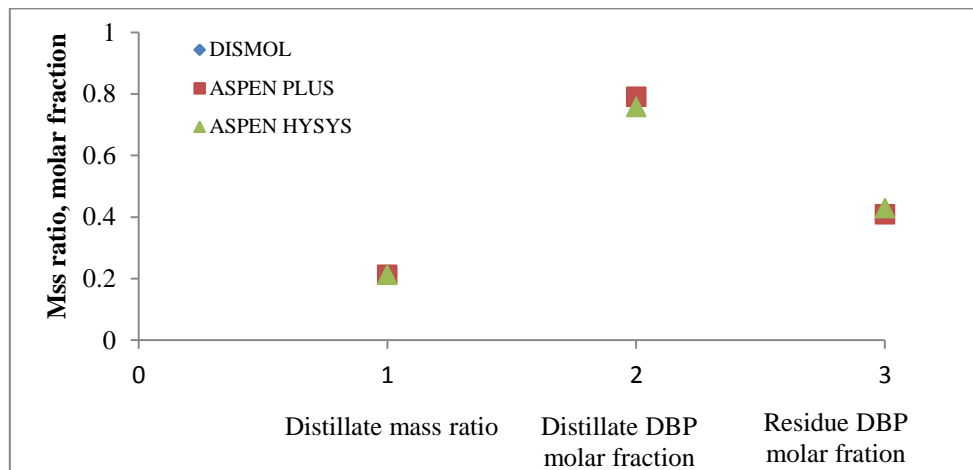


Fig. 1: The simulation results for DISMOL, ASPEN PLUS and Developed ASPEN HYSYS

It is clear that the results of ASPEN HYSYS simulation are comparable to those DISMOL and ASPEN PLUS in term of distillation mass ratio, distillate DBP molar fraction and residue DBP molar fraction. Hence, the ASPEN HYSYS simulator can be applied to any process related with MD such as MD for palm oil considered in this work.

The deodorization of refined palm oil process is simulated via ASPEN HYSYS model developed following the procedure outlined in [9] and validated with patent of Refining of edible oil rich in natural carotenes [11]. The results were found to be in good agreement for each simulation results which efficiency errors are less than 3% [10].

In the past, ANN based models have been considered as possible alternatives to predict process behaviors with molecular distillation and crude oil distillation [7, 12-14]. In this work ANN models based on 3 inputs and 2 inputs are constructed to facilitate operational optimization of MD in deodorization of refined palm oil process. The architectures of neural networks (NN) are investigated by studying the effect of layers, hidden layers and number of neurons in each layer. Transfer function for NN performance is also examined to give the best predictions for NN architecture. The resulting model is then incorporated in optimization to determine the operating conditions in MD column that maximize the quality of palm oil. Note, ASPEN HYSYS model is used to generate input-out data of the process to be used in ANN model.

Finally, the contribution and the novelty of this work have been highlighted as:

- Falling film molecular distillation (MD) model for refined palm oil process has been developed from the single flash vessel in ASPEN HYSYS simulator. Since, there is no module available in the ASPEN HYSYS simulator, developed MD simulation has been validated with patent's data of refining of edible oil rich in natural carotene. The simulation results are in good agreement with those of the patent.
- The required data for developing ANN model is generated via simulation of the developed MD model using ASPEN HYSYS simulator. Even though, there are many literatures on the simulation of MD, the MD model for deodorization of palm oil process has not been carried out before.

2. MD Process for the Palm Oil

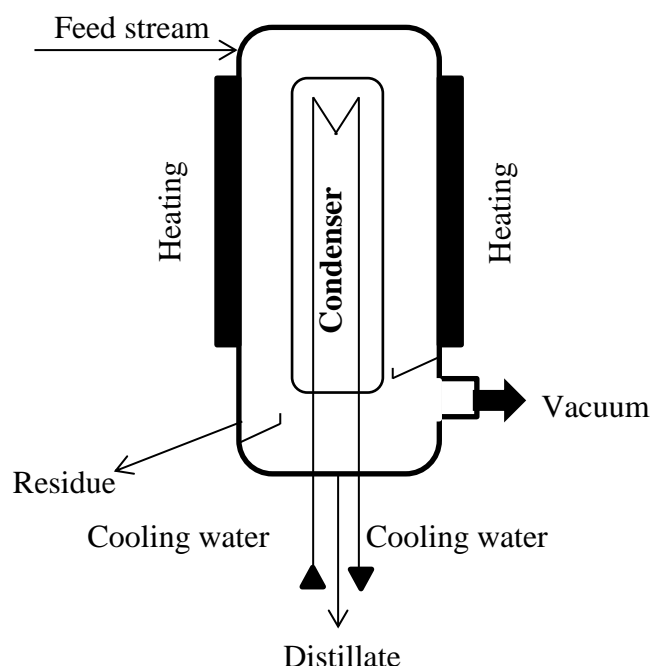


Fig. 2: Schematic Diagram of a Molecular distillation process

A process for production of palm oil consists of 3 main parts, which are degumming, bleaching and deodorization. Degumming is a process of removing phosphatide from crude oil, and then the degummed oil is treated by bleaching earth before entering the deodorization column. Schematic diagram of MD is shown in (fig. 2). The MD column mainly consists of evaporator and internal condenser. In the MD column, high vacuum is achieved by vacuum booster pump. The liquid from feed stream is degassed by degasser unit and then enter the heated evaporator [15]. The heated liquid enters the MD as vapor phase. Each molecule has different moving distance; light molecule has longer mean free path than the heavy molecule. The longer mean free path provides more capability for molecule to reach the condenser board. The lighter molecule will condense and leave the column through the distillate stream. However, the heavy molecule will leave via the residue stream. In this work, beta-carotene and tocopherol are heavy substances; they will leave the MD column through the residue stream, whereas free fatty acid is lighter and leaves the MD column through the distillate stream. Usually feed flow rate (F), column temperature (T) and pressure (P) influence the output concentration of beta-carotene, tocopherol and free fatty acid. The product quality

(beta-carotene and tocopherol concentration at residue) increases with decreasing temperature, on the other hand with increasing pressure, according to (equation 1.)

$$\lambda = \frac{RT}{\sqrt{2}\pi d^2 N_A P} \quad (1)$$

Where λ is the mean free path, R is gas constant, T is temperature, P is the pressure, N_A is Avogadro's number and d is molecular diameter.

Mean free path is function of both temperature and pressure. Increasing temperature increases the mean free path; thus the heavy molecules (beta-carotene and tocopherol) can more easily reach the condenser. Consequently, they leave the column through the distillate stream; hence, the quality of edible oil is decreased. But the effect of pressure is opposite; the heavy molecules cannot more easily reach the condenser, therefore product quality is increased.

With the increasing feed flow rate, the product quality decline. Increasing feed flow rate results in shorter residence time. The lighter molecule (FFA) could not evaporate timely, and therefore, it remains in the residue. Consequently, the quality of edible oil decreases because the FFA contaminates the residue stream.

3. ANN modeling

Artificial neural network (ANN) is widely accepted as alternative technique to capture and represent the complicated input and output relationship of processes [16]. It is an information processing system that does not have to be programmed and non-algorithmic. ANN models are applied in various applications such as process control, system identification, business, modeling, pattern recognition and simulation. It performs intellectual tasks similar to human brain by acquires knowledge during learning and stores within inner neuron. The significance of using neural network is in its easy to perform feature for developing a process model. Since the process is nonlinear, so it is difficult to solve manually. Conversely, the first principle modeling requires knowledge to calculate physical properties for developing model. In addition, neural network model is less computationally expensive than 1st principle model. The neural network consists of neurons in different layers within the network, which are input layer, one or more hidden layers and output layer. The neuron network essentially receives input data (signal), train and processes then sends outputs signal. Each input is weighted, and its weight (w) is relying on the particular input. The weights and biases (b) are the connection among input, neurons and outputs of the neural

network. The weights and biases are then summed and added up by a transfer function into one or more outputs depending on the process.

3.1 Neural network architecture and training

In this study, feed forward network is used to solve the approximation fitting problem. Multi-layer perceptron (MLP) network is the most common and famous type of feed forward network. Feed forward network is a straight forward network that travel only one way (no feedback loop), and it is a supervisory network that requires outputs in order to learn. The architecture of neural network for multi-input and multi- output is shown in Fig. 3, where i is number of elements in input, and j is number of neurons in layer. The summation of weight inputs (wx) with biases (b) are the argument of transfer function (f); hyperbolic tangent sigmoid transfer function (*tansig*) and linear transfer function (*purelin*), which produces the output (y). In addition, the outputs of each transitional layer are the input of the subsequent layer.

Back propagation algorithm based on Levenberg-Marquardt (*trainlm*) is the training function used in order to train the network [17]. This algorithm is the most commonly used procedure to determine the error derivative of the weight. Before starting the network design, it is important to ensure that the training data cover the range of input space. It is because the neural network is skillful in interpolation rather than extrapolation of data [18, 19].

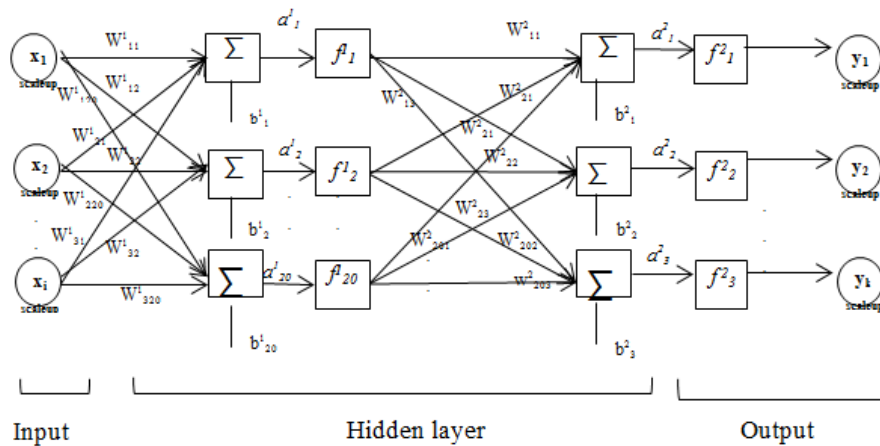


Fig. 3: Neural network architecture for 1st ANN model

The output variables of the 1st ANN model can be calculated and written as:

$$y_{k \text{ scaleup}} = f^2(a_k^2) \quad (2)$$

$$a_k^2 = (\sum_{j=1}^{20} w_{jk}^2 \times f^1(a_j^1)) + b_k^2 \quad (3)$$

$$a_j^1 = (\sum_{i=1}^3 w_{ij}^1 \times x_i) + b_j^1 \quad (4)$$

Where

i is the number of input variables.

j is the number of neurons.

k is the number of output variables.

a^1 and a^2 are linear combiner outputs of 1st hidden layer and outputs layer respectively.

b^1 and b^2 are the bias of 1st hidden layer and output layer respectively.

w^1 and w^2 are the synaptic weight of neuron for 1st hidden layer and output layer respectively.

f^1 is transfer function for hidden layer.

f^2 is transfer function for output layer.

Lastly, the output values are calculated or de-normalized to the original units by equation

$$y_k = (y_{k \text{ scaleup}} \times y_{k \text{ std}}) + y_{k \text{ mean}} \quad (5)$$

Where

y_k = output variables

$y_{k \text{ scaleup}}$ = scaleup output variables

$y_{k \text{ std}}$ = standard deviation of scaleup output variables

$y_{k \text{ mean}}$ = average of scaleup output variables

An effective ANN model can be developed if the design variables and its responses are normalized. The input variables and output variable are normalized before training in order to avoid the over fitting. The input data are normalized and scaled up as follows

$$\begin{matrix} x_{1 \text{ scaleup}} \\ x_{2 \text{ scaleup}} \\ x_{3 \text{ scaleup}} \end{matrix} = \begin{pmatrix} \text{Feed flow rate scaleup} \\ \text{Temperature scaleup} \\ \text{Pressure scaleup} \end{pmatrix}$$

Where

i is number of input variables

The normalized output variables in the neural network correlation are as follows:

$$\begin{aligned}
& \begin{matrix} Y_1 \text{ scaleup} \\ Y_2 \text{ scaleup} \\ Y_3 \text{ scaleup} \end{matrix} = \begin{pmatrix} \text{Beta-carotene scaleup} \\ \text{Tocopherol scaleup} \\ \text{Free fatty acid scaleup} \end{pmatrix} \\
& x_{i \text{ scaleup}} = \frac{x_i - x_{i \text{ mean}}}{x_{i \text{ std}}} \quad (6)
\end{aligned}$$

Where $x_{i \text{ mean}}$ is the average of input variables.
 $x_{i \text{ std}}$ is the standard deviation of input variables,

The standard deviation of each input variable is calculated as follows:

$$x_{i \text{ std}} = \sqrt{\left(\frac{\sum (x_i - x_{i \text{ mean}})^2}{n-1} \right)} \quad (7)$$

Where n is total number of data
 i is input variables

The normalization of data accelerates the training process, and also improves capabilities of the network [20].

Sensitivity analysis or input variable analysis is used and applied in this part as a technique to eliminate the least impact on the process. It is a technique that assists by focusing only on significant effect of input variables to the process. In this part, a partial modeling is applied to estimate the sensitivity of predicted responses. Varying pressure and temperature have largest effects on the outputs; nevertheless, feed flow rate has less effect on any of outputs. It can be concluded that x_2 and x_3 are significant variables, whereas x_1 is insignificant variable.

Later, in this work, we develop 2 difference models; the first ANN model (1st ANN) based on 3 inputs (x_1, x_2, x_3) and 3 outputs: concentration of beta-carotene and tocopherol at residue and free fatty acid at distilled stream (y_1, y_2, y_3) and the second ANN model (2nd ANN) based on 2 inputs (x_2, x_3) without considering insignificant variable and 3 outputs (y_1, y_2, y_3). The ANN model is developed and the effects of numbers of neuron and hidden layer are discussed. In this study different inputs are generated from the ASPEN HYSYS simulation of refined palm oil process to be used to develop the artificial neural network (ANN) models. The 70% of input data are used for training (bold), 15% data are used for

testing (normal) and the remaining 15% data (italic) are used for validation (Table C, Appendix). The training, testing, and validation is executed to estimate the performance of neural network [21] for forecasting the concentration of beta-carotene (y_1), tocopherol (y_2), and free fatty acid(y_3), in order to estimate the quality of edible oil, in terms of value added and contaminant. The input variables and its statistics for the first ANN model and second ANN model are shown in Table 1 and 2 respectively. The feed flow rate for first model is in the range of 1000-2000 kg/hr, for both models, temperature and pressure are in the range of 100-200°C and 0.00000-0.001 kPa respectively.

Table1

Statistical data for input variables and its output for 1st ANN model.

	MEAN	STD	Variables range	Scaleup range
Feed flow rate (kg/hr)	1500	409.49	1000-2000	-1.221-1.221
Column Temperature (°C)	150	35.46	100-200	-1.410-1.410
Column Pressure (kPa)	0.0005	0.000317	0-0.001	-1.576-1.576
Beta-carotene in residue (mass fraction)	3.88×10^{-4}	0.000208	1.166×10^{-6} - 5.6×10^{-4}	-1.850-0.848
Tocopherol in residue (mass fraction)	6.27×10^{-4}	0.000343	1.53×10^{-6} - 9.10×10^{-4}	-1.82-0.0826
Free fatty acid in distillate (mass fraction)	6.54×10^{-1}	0.384413	0.061-1.00	-1.54-0.901

Table 2

Statistical data for input variables and its outputs for 2nd ANN model.*

	MEAN	STD	Variable s range	Scaleup range
Column Temperature (°C)	150	35.68	100-200	-1.410-1.410
Column Pressure (kPa)	0.0005	0.000319	0-0.001	-1.576-1.576
Beta-carotene in residue (mass fraction)	3.88×10^{-4}	0.000209	1.166×10^{-6} - 5.6×10^{-4}	-1.850-0.848
Tocopherol in residue (mass fraction)	6.27×10^{-4}	0.000345	1.53×10^{-6} - 9.10×10^{-4}	-1.82-0.0826
Free fatty acid in distillate (mass fraction)	6.54×10^{-4}	0.386778	0.061-1.00	-1.54-0.901

*without considering feed flow rate

4. Results and discussion

The number of neurons and layer are varied as shown in Table 3-4. The Mean square error (MSE) is the measure of performance for the network, and the best ANN model is based on the least mean square error. The network is trained, validated and tested by neural network tool (*nntool*) in Matlab toolbox.

4.1 The effect of number of layers

The number of layer for 1st ANN and 2nd ANN model is investigated with fixed 10 neurons. The effect of number of layers is shown in Tables 3-4. Increasing number of layers from 3 to 10 with fixed number of neurons results in inaccuracy. The training is terminated at

sufficiently small value of the mean square error (MSE). They show that 2 and 3 layers network has smaller MSE compared to others. The smallest MSE is for 2 layers network, it gives very good values of the correlation data, and the training is stopped after 15 iteration (epoch) and 12 iteration for 1st ANN and 2nd ANN models respectively. However, increasing the number of layers results in inaccurate predictions.

Table 3
Effect of number of layers on the network performance (1st ANN model)

	2 layers	3 layers	10 layers
MSE	0.0125	0.4230	4.3700
Epoch	15	17	6

Table 4
Effect of number of layers on the network performance (2nd ANN model)

	2 layers	3 layers	10 layers
MSE	0.0287	0.0445	1.5138
Epoch	12	21	23

4.2 The effect of number of neurons

Having found out that the 2 layer network is the best, the effect of number of neurons is investigated for this network (1 hidden layer and 1 output layer). The number of neurons is varied from 1 to 25 neurons. The transfer functions used in this work are *tansig* (hyperbolic tangent sigmoid transfer function) for the first layer and *purelin* (a linear transfer function) for the second layer. The results for 1st and 2nd ANN model are summarized in Figs 4-5. The optimum number of neurons for 2 layers network are 20 neurons for both models.

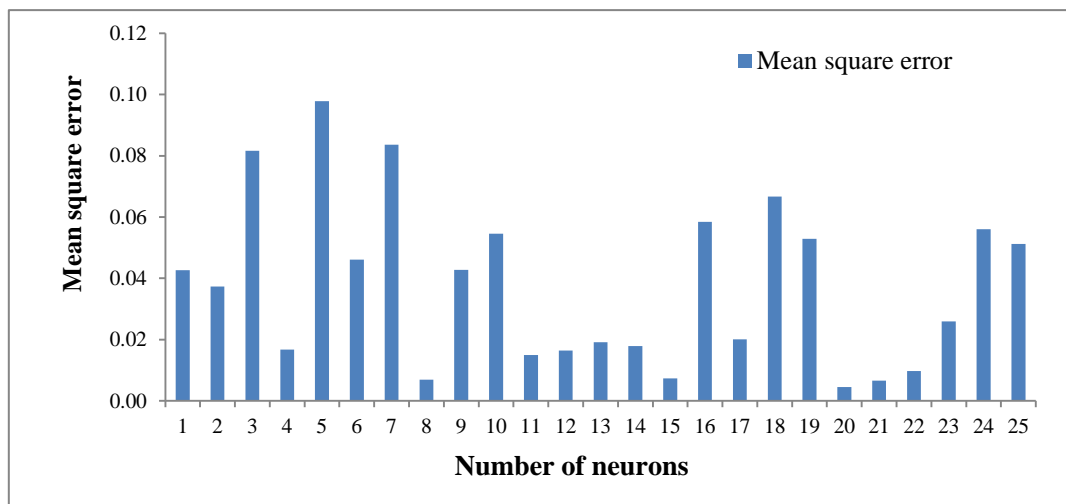


Fig. 4: Validation MSE response for 1st ANN model with 2 layers

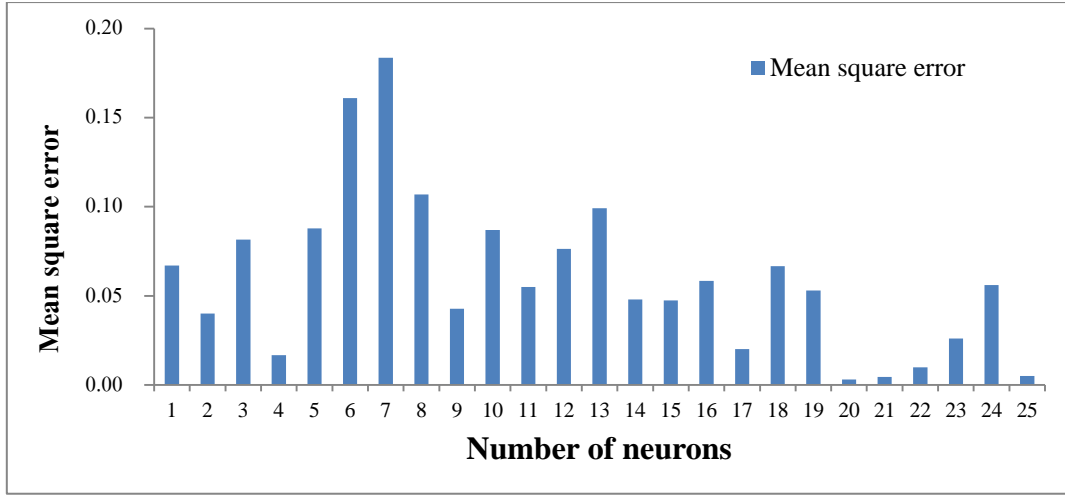


Fig. 5: Validation MSE response for 2nd ANN model with 2 layers (without considering feed flow rate)

Figs. 6-7 show the optimum regression plot of training, validation and testing for 1st ANN model and 2nd ANN model respectively. They show the relationship between the network target and the output. It can be seen that, the regression is nearly equal to 1, which is desirable. However, the performance evaluation of 20 neurons configuration is the best although the 20 neurons network take longer iteration time to reach a target. The optimum weight and bias for the 1st ANN model with 2 layers for 20 neurons are shown in Tables A, and Tables B in appendix shows weight and bias for the 2nd ANN model with 2 layers and 20 neurons.

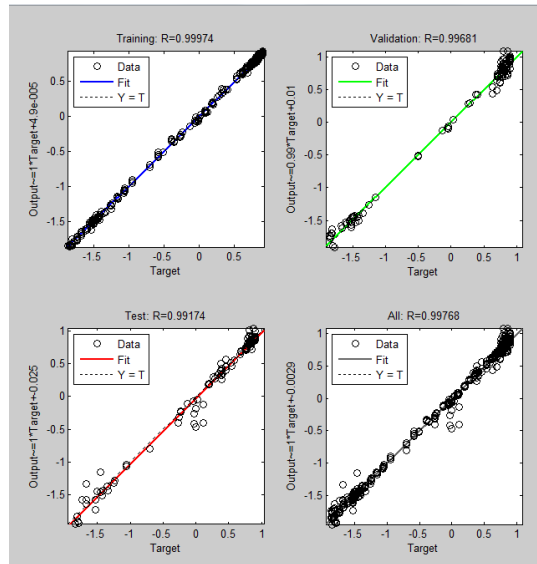


Fig. 6: The regression plot of training, validate, testing and the overall regression for 20 neurons (1st ANN model)

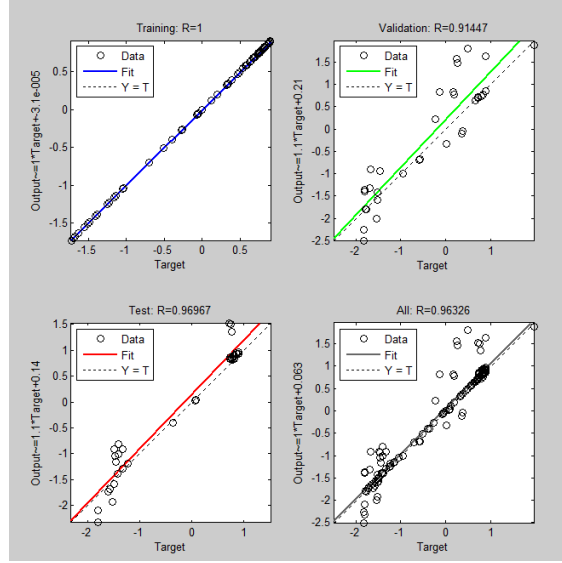


Fig. 7: The regression plot of training, validate, testing and the overall regression for 20 neurons (2nd ANN model)

4.2 ANN generalization

Neural networks with 2 layers (1 hidden layer and 1 output layer) and 20 neurons are used to predict the outputs of beta-carotene and tocopherol at residue and free fatty acid at distillate stream. The input data to predict the outputs are the data that have not been used before for training, validation and testing. The 1st ANN model predicts the outputs concentration at different F , T and P values that are outward the training, testing and validation data, which are at 1100 kg/hr, 140°C and 0.00055 kPa respectively. The 2nd ANN model is also investigated at different T and P of 140°C and 0.00055 kPa respectively (T and P values are same those used in the 1st ANN model). The results based on ANN are compared with ASPEN HYSYS simulator as shown in Figs 8-22.

At constant F and T (Figs. 8-10), predicted outputs of 1st ANN model are found to be close to those predicted by ASPEN HYSYS simulator. The criteria used for evaluation is R-square (R^2) as follows:

$$R^2 = 1 - \frac{\sum_{i=1}^n (y_{p,i} - y_{o,i})^2}{\sum_{i=1}^n (y_{o,i} - \bar{y}_o)^2} \quad (8)$$

Where $y_{p,i}$ is correlated value; $y_{o,i}$ is observed value; \bar{y}_o is average observed value and R^2 is a statistical measure used to measure the linear correlation between correlated and measured value. The R^2 of predicted outputs is 0.9. Also, prediction outputs of 2nd ANN model at constant T (Figs. 11-13) is found to be close to those predicted by ASPEN HYSYS

simulator but with R^2 equal to 0.99 for all outputs. According to these (Figs. 8-13), elevated pressure results in improved prediction of the outputs by both 1st and 2nd ANN models. It is important to note that the high pressure in MD column influences to shorter mean free path of molecules (equation 1). The shorter mean free path offers less capability for molecules to travel or reach the condensation board, therefore, less vaporization occurs. Consequently, it increases the quality of edible oil.

At constant F and P (Figs. 14-16), the 1st ANN model displays accurate prediction with R^2 equal to 0.99 for all outputs. Also, at constant P , the 2nd ANN model also predicts precise outputs with R^2 equal to 1 as shown in (Figs 17-19). These figures clearly show that the predicted outputs decrease with increasing temperature. The increasing T unfortunately reduces the concentration of beta-carotene and tocopherol and they are vaporized to distillate stream. It is necessary to note that high temperature operation not only reduces the concentration of beta-carotene and tocopherol but also destroys them due to temperature sensitivity. Thus, high temperature reduces palm oil quality.

Figs. 20-22 depict the predicted outputs of 1st ANN model and ASPEN HYSYS simulator at constant T and P . The concentrations of beta- carotene and tocopherol at residual stream and free fatty acid at distillate show no significant difference. The R^2 of 1st ANN model prediction and that with ASPEN HYSYS simulator are both equal to 1. However, varying feed flow rates (different residence time) shows no significant differences (observed by both ANN model and ASPEN HYSYS simulator).

The predictions by 2 different ANN models follow the expected prediction of ASPEN HYSYS simulator. Lastly, these studies reveal that the proposed artificial neural networks with 2 layer (1 hidden layer and 1 output layer) and 20 neurons in hidden layer are able to predict the concentration of beta-carotene, tocopherol at residue and free fatty acid at distillate accurately.

Moreover, it can be clearly seen that the prediction output of 1st ANN model is more accurate than 2nd ANN model. The next section focuses on the optimization of process design based on optimum model.

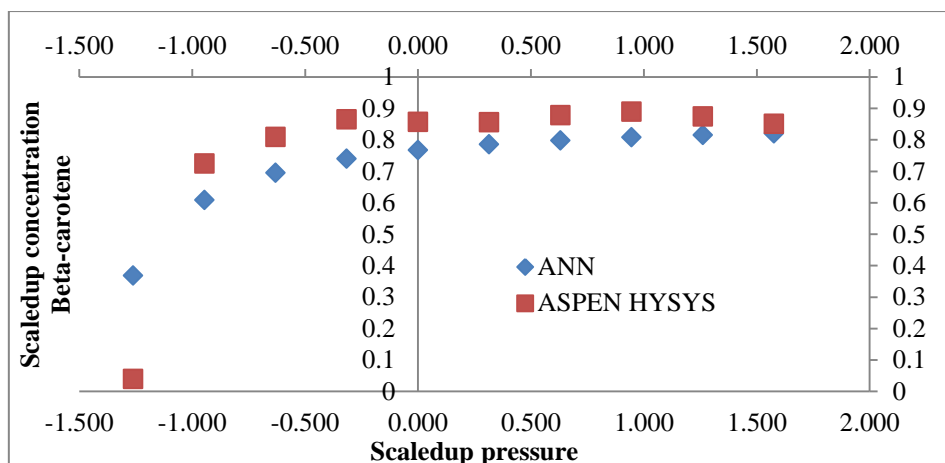


Fig. 8: Predicted outputs of beta-carotene for 1st ANN model at constant feed flow rate (1100 kg/hr) and temperature (140 °C).

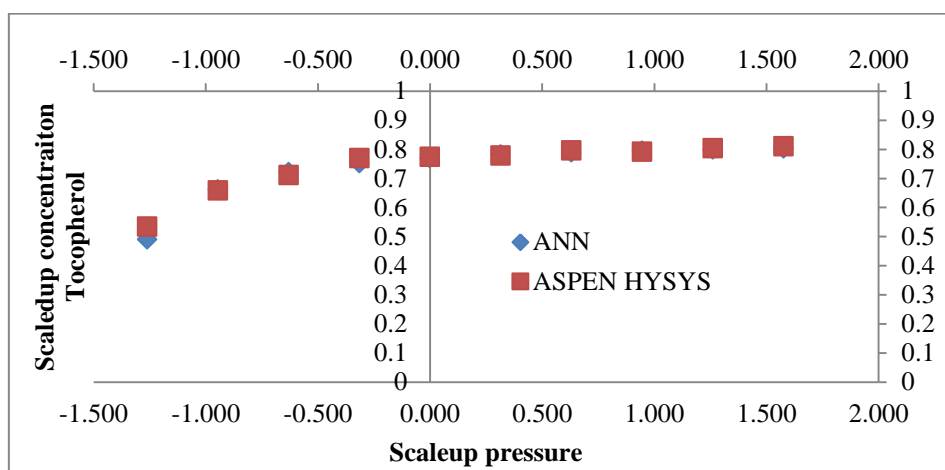


Fig. 9: Predicted outputs of tocopherol for 1st ANN model at constant feed flow rate (1100 kg/hr) and temperature (140 °C).

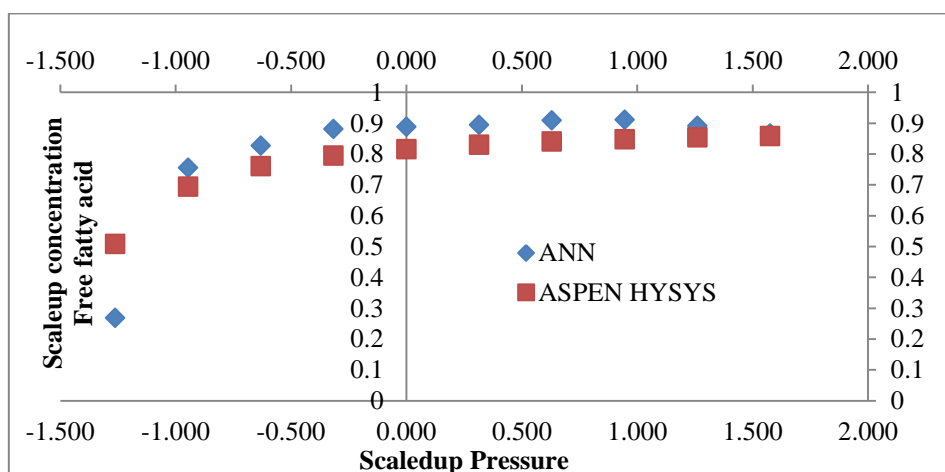


Fig. 10: Predicted outputs of free fatty acid for 1st ANN model at constant feed flow rate (1100 kg/hr) and temperature (140 °C).

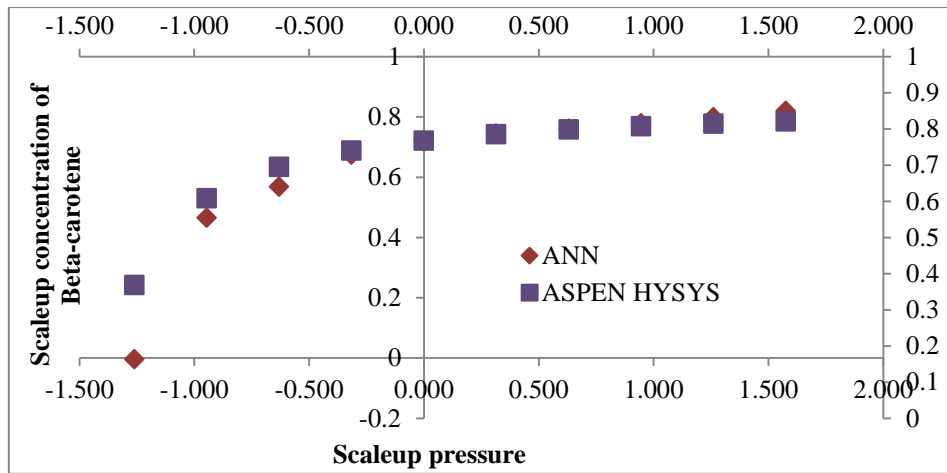


Fig. 11: Predicted outputs of beta-carotene for 2nd ANN model at constant temperature (140 °C).

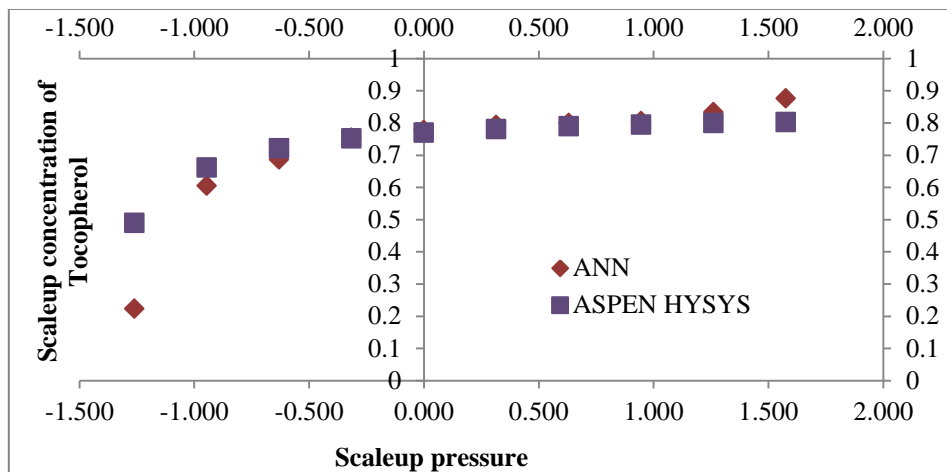


Fig. 12: Predicted outputs of tocopherol for 2nd ANN model at constant temperature (140 °C).

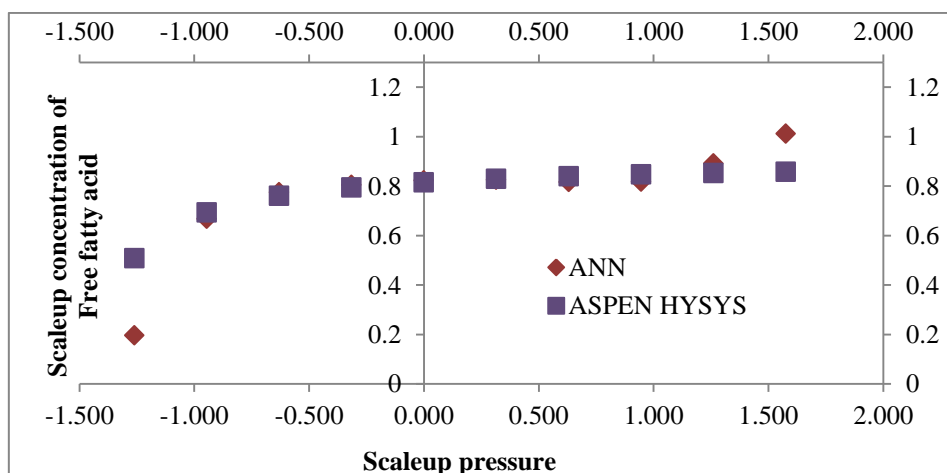


Fig. 13: Predicted outputs of free fatty acid for 2nd ANN model at constant temperature (140 °C).

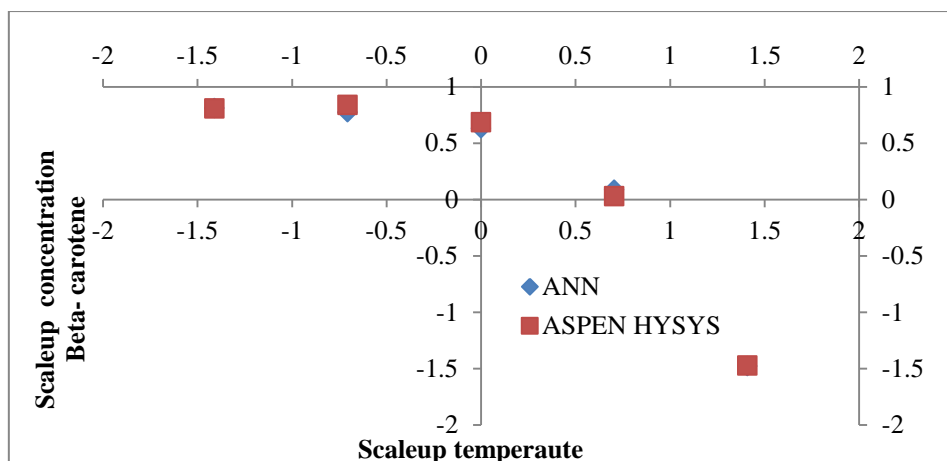


Fig. 14: Predicted outputs of beta-carotene for 1st ANN model at constant feed flow rate (1100 kg/hr) and pressure (0.00055 kPa)

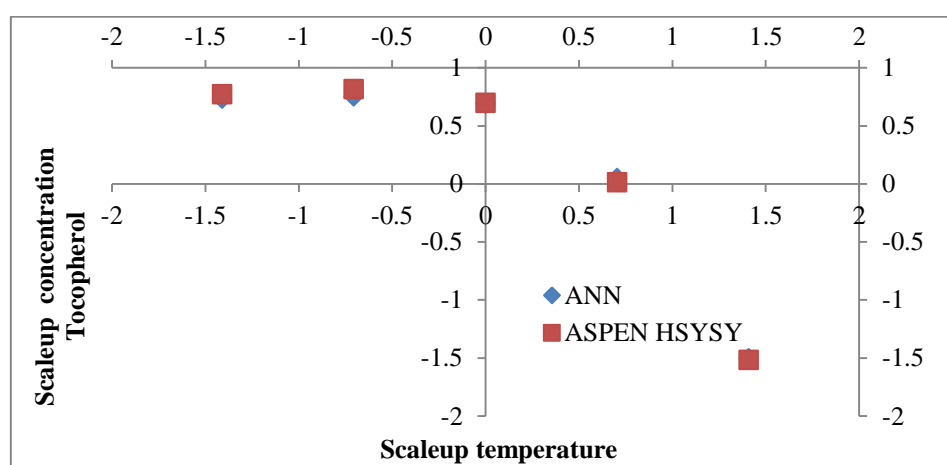


Fig. 15: Predicted outputs of tocopherol for 1st ANN model at constant feed flow rate (1100 kg/hr) and pressure (0.00055 kPa)

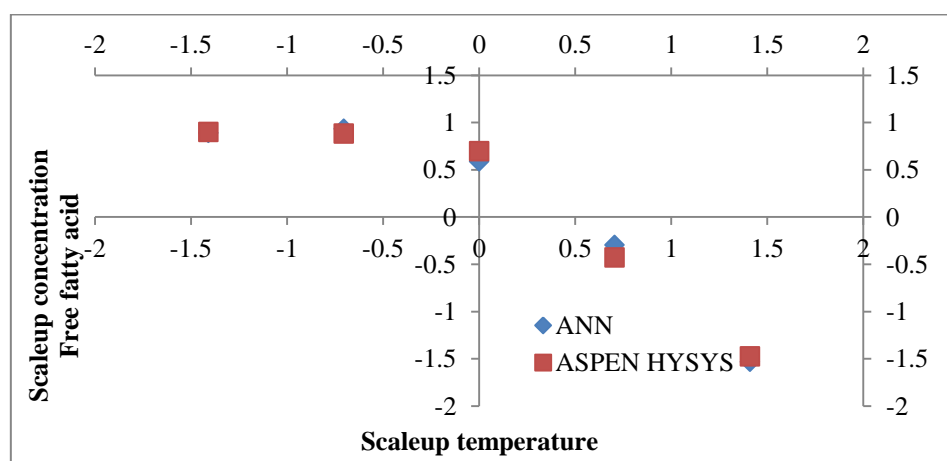


Fig. 16: Predicted outputs of free fatty acid for 1st ANN model at constant feed flow rate (1100 kg/hr) and pressure (0.00055 kPa)

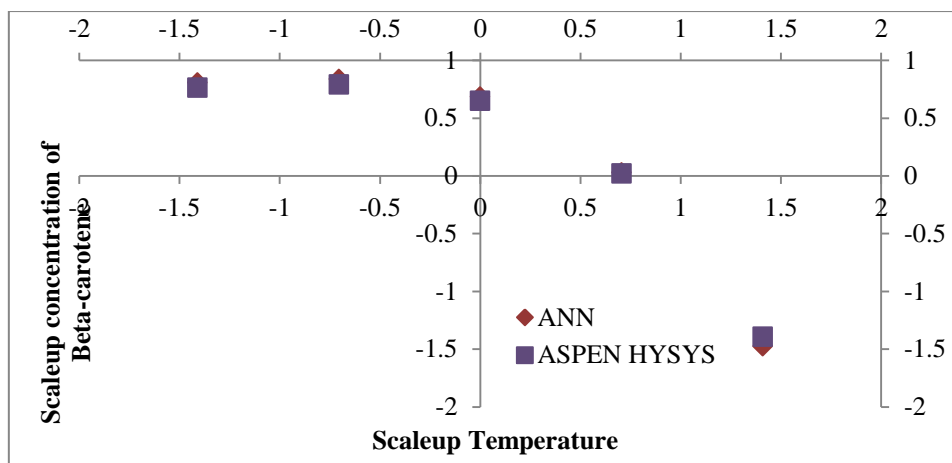


Fig. 17: Predicted outputs of beta-carotene for 2nd ANN model at constant pressure (0.00055 kPa)

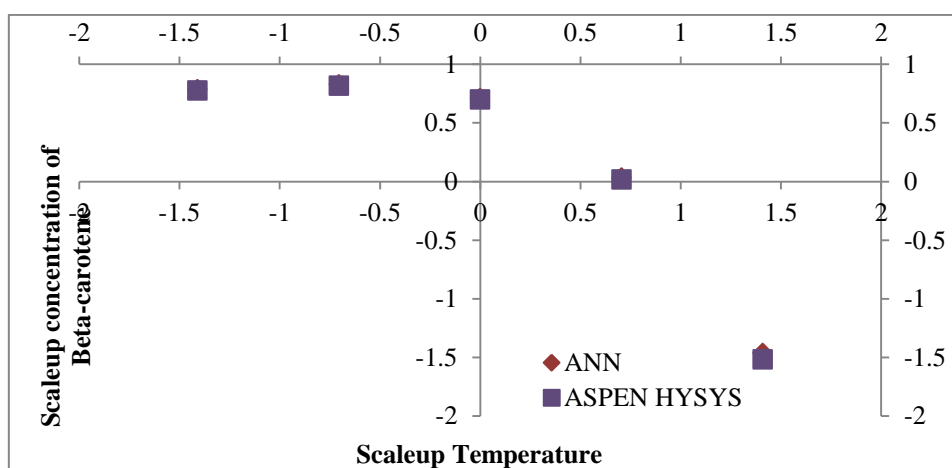


Fig. 18: Predicted outputs of tocopherol for 2nd ANN model at constant pressure (0.00055 kPa)

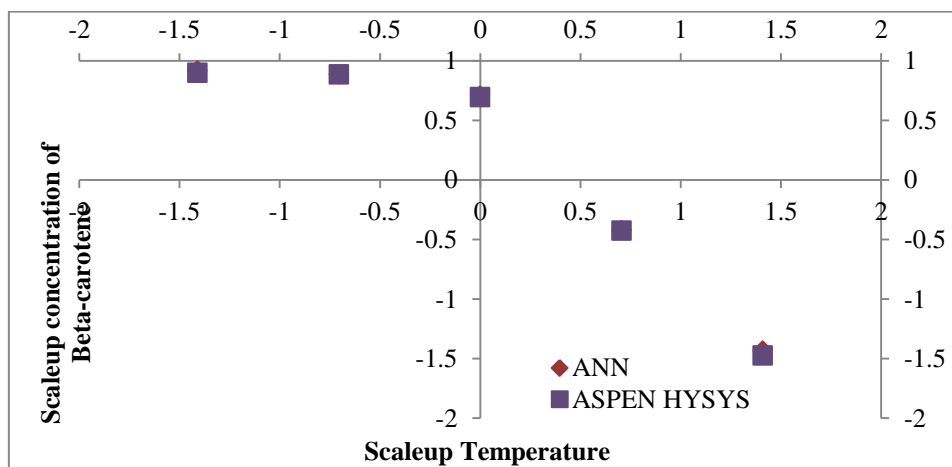


Fig. 19: Predicted outputs of free fatty acid for 2nd ANN model at constant pressure (0.00055 kPa)

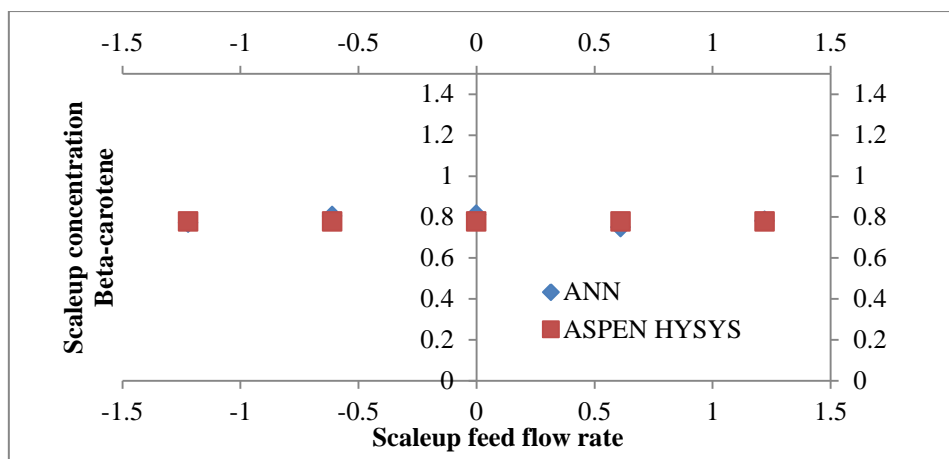


Fig. 20: Predicted outputs of beta-carotene for 1st ANN model at constant temperature (140 °C) and pressure (0.00055 kPa)

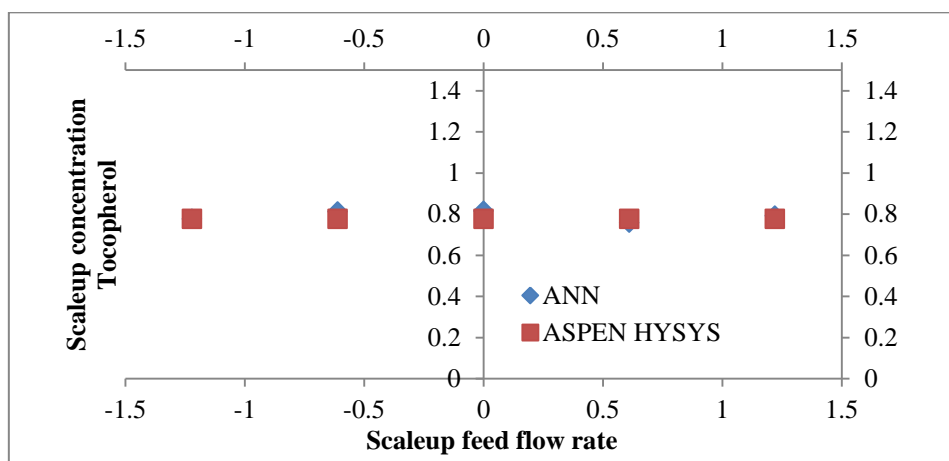


Fig. 21: Predicted outputs of free fatty acid for 1st ANN model at constant temperature (140 °C) and pressure (0.00055 kPa)

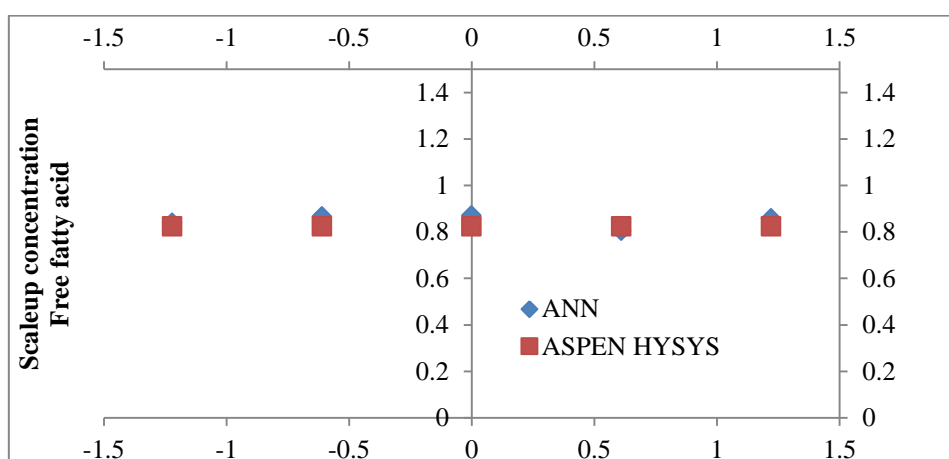


Fig. 22: Predicted outputs of free fatty acid for 1st ANN model at constant temperature (140 °C) and pressure (0.00055 kPa)

4.3 Optimization of MD for refined palm oil process based on optimum ANN model

In this section, the aim is to find the optimum parameters of feed flow rate (x_1), column temperature (x_2) and column pressure (x_3) that maximize the quality of edible oil, which depends on the recovery of beta-carotene (y_1) and tocopherol (y_2) in the residue and contaminant removal of free fatty acid (y_3) in the distillate. Maximization of the summation of these (Equation 9) maximizes the quality of the oil. The mathematical model of the process (Equation 9) is based on scaled-up ANN model. The upper bound and lower bound of variables are specified based on values in Table 1.

$$\text{Maximize:} \quad f(y) = y_{1 \text{ scaleup}} + y_{2 \text{ scaleup}} + y_{3 \text{ scaleup}} \quad (9)$$

$$\text{Subject to} \quad y_{k \text{ scaleup}} = \text{Purelin}(a_k^2)$$

$$a_k^2 = (\sum_{j=1}^{20} w_{jk}^2 \times \text{tansig}(a_j^1)) + b_k^2 \quad ; k = 1 - 3$$

$$a_j^1 = (\sum_{i=1}^3 w_{ij}^1 \times x_{i \text{ scaleup}}) + b_j^1 \quad ; j = 1 - 20$$

$$-1.221 \leq x_{1 \text{ scaleup}} \leq 1.221$$

$$-1.4099 \leq x_{2 \text{ scaleup}} \leq 1.4099$$

$$-1.5763 \leq x_{3 \text{ scaleup}} \leq 1.5763$$

Where

i is the number of input variables.

j is the number of neurons.

k is the number of output variables.

a^1 and a^2 are linear combiner outputs of 1st hidden layer and outputs layer respectively.

b^1 and b^2 are the bias of 1st hidden layer and output layer respectively.

w^1 and w^2 are the synaptic weight of neuron for 1st hidden layer and output layer respectively.

tansig is Tansig transfer function.

Purelin is Purelin transfer function.

$y_{k \text{ scaleup}}$ is scaleup of output variables in output layer.

$$y_{k \text{ scaleup}} = \begin{cases} y_{1 \text{ scaleup}} = \text{Beta carotene concentration scaleup} \\ y_{2 \text{ scaleup}} = \text{Tocopherol concentration scaleup} \\ y_{3 \text{ scaleup}} = \text{FFA concentration scaleup} \end{cases}$$

The optimization is carried out through solver add in in Microsoft Excel. The solution method used for this work is evolutionary which is for nonlinear non-smooth equation. The optimum results of F , T , P , their scaled-up values and the responses of beta-carotene tocopherol, free fatty acid and their real values are shown in Table 5. The real values are de-normalized values based on equation 5-7.

Table 5

The optimum variables and optimum predicted responses from 1st ANN model and ASPEN HYSYS simulator

Optimum value	Input			Output		
	Feed flow rate (x_1)	Temperature (x_2)	Pressure (x_3)	Beta-carotene (y_1)	Tocopherol (y_2)	Free fatty acid (y_3)
Scaleup	0.434	-0.212	0.749	1.054	1.062	1.023
Real value	1677	142	0.00073	0.000607	0.000990	1
ASPEN	1677	142	0.00073	0.000553	0.000896	0.972524

The optimum results of F , T and P are found to be 1677 kg/hr., 142 °C and 0.00073 kPa respectively. The response results from 1st ANN model and ASPEN HYSYS simulator are shown in Table 5 and the statistical regression of data is shown in Table 6. It can be seen that the optimization result from 1st ANN model is close to the result from ASPEN HYSYS simulator with R^2 equal to 1, and standard error of 9.60×10^{-6} .

Table 6

The regression statistic of 1st ANN and ASPEN HYSYS simulator

Regression Statistics	
Multiple R	1
R Square	1
Adjusted R Square	1
Standard Error	9.60×10^{-6}
Observations	3

Lastly, optimum F , T and P values by 1st ANN model is found to be around 1667 kg/hr, 142°C and 0.00073 kPa respectively. The regression statistics of neural networks show good agreement with the results from the ASPEN HYSYS simulator. Moreover, Operating under optimal condition based ANN model, percent recovery of product nutrients is higher than 90% in this work.

5. Conclusion

Two Neural networks based correlations for refined palm oil process to predict the concentration of beta-carotene, tocopherol and FFA are developed. Feed forward back propagation is used to determine the optimum architecture for the 1st ANN model (based on 3 inputs: F , T and P) and the 2nd ANN model (based on 2 inputs: T and P). The effect of number of layers and neurons are studied for both models. It is found that 2 layers and 20 neurons are optimum of ANN structures for both ANN models. *Tansig* and *purelin* are the best predicted transfer function for these neural network architectures. The proposed ANN models are capable of predicting the concentrations of beta-carotene, tocopherol and free fatty acid very close to those obtained by ASPEN HYSYS simulator. It is found that increasing temperature leads to decrease quality of edible oil however, increasing pressure leads to increase the quality of edible oil.

In addition, optimizations based on optimum ANN model is performed, and the results show that the optimum F , T and P are at 1677 kg/hr., 142^oC and 0.00073 kPa respectively. Lastly it can be concluded that ANN can be successfully applied for refined palm oil process with a very good accuracy.

Acknowledgement

The authors would like to acknowledge the Prince of Songkla Universit, Songkhla, Thailand for providing financial support to Mrs. Noree Tehlah for carrying out this research abroad and the School of Engineering, University of Bradford, UK for providing research facilities and facilitators, which make this complete and successful study.

References

1. Li, Y. and S.-L. Xu, *DSMC simulation of vapor flow in molecular distillation*. Vacuum, 2014. **110**: p. 40-46.
2. Jung, J., et al., *Optimal operation strategy of batch vacuum distillation for sulfuric acid recycling process*. Computers & Chemical Engineering, 2014. **71**: p. 104-115.
3. Huang, H.-J., et al., *A review of separation technologies in current and future biorefineries*. Separation and Purification Technology, 2008. **62**(1): p. 1-21.
4. Casilio, D., N. T. Dunford. Nutritionally enhanced edible oil and oilseed processing. 178-192 Canada, AOCS Press., 2004.
5. Wang, A., et al., *Process optimization for vacuum distillation of Sn–Sb alloy by response surface methodology*. Vacuum, 2014. **109**: p. 127-134.
6. Chen, F., et al., *Optimizing conditions for the purification of crude octacosanol extract from rice bran wax by molecular distillation analyzed using response surface methodology*. Journal of Food Engineering, 2005. **70**(1): p. 47-53.
7. Shao, P., S.T. Jiang, and Y.J. Ying, *Optimization of Molecular Distillation for Recovery of Tocopherol from Rapeseed Oil Deodorizer Distillate Using Response Surface and Artificial Neural Network Models*. Food and Bioproducts Processing, 2007. **85**(2): p. 85-92.
8. Wu, W., C. Wang, and J. Zheng, *Optimization of deacidification of low-calorie cocoa butter by molecular distillation*. LWT - Food Science and Technology, 2012. **46**(2): p. 563-570.
9. Mallmann, E.S., et al., *Development of a Computational Tool for Simulating Falling Film Molecular Design*. Computer Aided Chemical Engineering, 2009. **26**: p. 743-748.
10. Tehlah, N., *Simulation of Refined Palm Oil Process by ASPEN HYSYS*, Technical Report., Prince of Songkla University, 2015.
11. Unnikrishnan, R., *Refining of edible oil rich in natural carotenes and vitamin E*, in United State Patent 2001.
12. Motlaghi, S., F. Jalali, and M.N. Ahmadabadi, *An expert system design for a crude oil distillation column with the neural networks model and the process optimization using genetic algorithm framework*. Expert Systems with Applications, 2008. **35**(4): p. 1540-1545.
13. Lluvia M., O.-E., M. Jobson, and R. Smith, *Operational optimization of crude oil distillation systems using artificial neural networks*. Computer & Chemical Engineering 2013. **59**: p. 178-185.
14. Osuolale, F.N., et al., *Multi-objective Optimisation of Atmospheric Crude Distillation System Operations Based on Bootstrap Aggregated Neural Network Models*. Computer Aided Chemical Engineering, 2015. **Volume 37**: p. 671-676.
15. Zereskhi, S., *Distillation - Advances from Modeling to Application*. 2012: InTech.
16. Mujtaba, I.M., A. Hussain, *Application of Neural Networks and Other Learning Technologies in Process Engineering*: Imperial College Press, 2001.
17. Hagan, M.T., H.B. Demuth, and M.H. Beale, *Neural Network Design*. 1996: PWS Publishing Company of international Thomson Publishing Inc., Boston.
18. Tanvir, M.S. and I.M. Mujtaba, *Neural network based correlations for estimating temperature elevation for seawater in MSF desalination process*. Desalination, 2006. **195**: p. 251-272.
19. Bareello, M., et al., *Neural network based correlation for estimating water permeability constant in RO desalination process under fouling*. Desalination, 2014. **345**: p. 101-111.
20. Mashaly, A.F., et al., *Predictive model for assessing and optimizing solar still performance using artificial neural network under hyper arid environment*. Solar Energy, 2015. **118**: p. 41-58.
21. Khayet, M. and C. Cojocaru, *Artificial neural network modeling and optimization of desalination by air gap membrane distillation*. Separation and Purification Technology, 2012. **86**: p. 171-182.

1. Li, Y. and S.-L. Xu, *DSMC simulation of vapor flow in molecular distillation*. Vacuum, 2014. **110**: p. 40-46.
2. Jung, J., et al., *Optimal operation strategy of batch vacuum distillation for sulfuric acid recycling process*. Computers & Chemical Engineering, 2014. **71**: p. 104-115.
3. Huang, H.-J., et al., *A review of separation technologies in current and future biorefineries*. Separation and Purification Technology, 2008. **62**(1): p. 1-21.
4. Casilio, D., N. T. Dunford. Nutritionally enhanced edible oil and oilseed processing. 178-192 Canada, AOCS Press., 2004.
5. Wang, A., et al., *Process optimization for vacuum distillation of Sn–Sb alloy by response surface methodology*. Vacuum, 2014. **109**: p. 127-134.
6. Chen, F., et al., *Optimizing conditions for the purification of crude octacosanol extract from rice bran wax by molecular distillation analyzed using response surface methodology*. Journal of Food Engineering, 2005. **70**(1): p. 47-53.
7. Shao, P., S.T. Jiang, and Y.J. Ying, *Optimization of Molecular Distillation for Recovery of Tocopherol from Rapeseed Oil Deodorizer Distillate Using Response Surface and Artificial Neural Network Models*. Food and Bioprocess Technology, 2007. **85**(2): p. 85-92.
8. Wu, W., C. Wang, and J. Zheng, *Optimization of deacidification of low-calorie cocoa butter by molecular distillation*. LWT - Food Science and Technology, 2012. **46**(2): p. 563-570.
9. Mallmann, E.S., et al., *Development of a Computational Tool for Simulating Falling Film Molecular Design*. Computer Aided Chemical Engineering, 2009. **26**: p. 743-748.
10. Tehlah, N., *Simulation of Refined Palm Oil Process by ASPEN HYSYS*, Technical Report., Prince of Songkla University, 2015.
11. Unnikrishnan, R., *Refining of edible oil rich in natural carotenes and vitamin E.*, in United State Patent 2001.
12. Motlaghi, S., F. Jalali, and M.N. Ahmadabadi, *An expert system design for a crude oil distillation column with the neural networks model and the process optimization using genetic algorithm framework*. Expert Systems with Applications, 2008. **35**(4): p. 1540-1545.
13. Lluvia M., O.-E., M. Jobson, and R. Smith, *Operational optimization of crude oil distillation systems using artificial neural networks*. Computer & Chemical Engineering 2013. **59**: p. 178-185.
14. Osuolale, F.N., et al., *Multi-objective Optimisation of Atmospheric Crude Distillation System Operations Based on Bootstrap Aggregated Neural Network Models*. Computer Aided Chemical Engineering, 2015. **Volume 37**: p. 671-676.
15. Zereszki, S., *Distillation - Advances from Modeling to Application*. 2012: InTech.
16. Mujtaba, I.M., A. Hussain, *Application of Neural Networks and Other Learning Technologies in Process Engineering*: Imperial College Press, 2001.
17. Hagan, M.T., H.B. Demuth, and M.H. Beale, *Neural Network Design*. 1996: PWS Publishing Company of international Thomson Publishing Inc., Boston.
18. Tanvir, M.S. and I.M. Mujtaba, *Neural network based correlations for estimating temperature elevation for seawater in MSF desalination process*. Desalination, 2006. **195**: p. 251-272.
19. Bareello, M., et al., *Neural network based correlation for estimating water permeability constant in RO desalination process under fouling*. Desalination, 2014. **345**: p. 101-111.
20. Mashaly, A.F., et al., *Predictive model for assessing and optimizing solar still performance using artificial neural network under hyper arid environment*. Solar Energy, 2015. **118**: p. 41-58.
21. Khayet, M. and C. Cojocaru, *Artificial neural network modeling and optimization of desalination by air gap membrane distillation*. Separation and Purification Technology, 2012. **86**: p. 171-182.



Noree Tehlah received the B.Sc. degree in chemical engineering from Universiti Teknologi Petronas (UTP), in Perak Malaysia in 2010. She is currently studying for combined degree of Master and PhD in chemical engineering at Prince of Songkla University (PSU), Thailand. Her current research interests include simulation, neural network and process control.



Pornsiri Kaewpradit, Asst. Prof. Dr. is Lecturer in Department of Chemical Engineering at Prince of Songkla University, Songkhla THAILAND. She got her Doctoral degrees in Chemical Engineering from Chulalongkorn University, financial supported by Royal Golden Jubilee (RGJ), The Thailand Research Fund (TRF). Her research area is on MODEL PREDICTIVE CONTROL (MPC) design, Mathematical and ANN modeling, Optimization and Process simulation through MATLAB and ASPEN/HYSYS, especially in Rubber and Energy Industries.



Iqbal M. Mujtaba is a Professor of Computational Process Engineering in the School of Engineering, at the University of Bradford. He obtained his BSc Eng and MSc Eng degrees in Chemical Engineering from Bangladesh University of Engineering & Technology (BUET) in 1983 and 1984 respectively and obtained his PhD from Imperial College London in 1989. He is a Fellow of the IChemE, a Chartered Chemical Engineer, and the Chair of the IChemE's Computer Aided Process Engineering Subject Group. Professor Mujtaba leads research into dynamic modelling, simulation, optimisation and control of batch and continuous chemical processes with specific interests in distillation, industrial reactors, refinery processes, desalination and crude oil hydrotreating focusing on energy and water. He has managed several research collaborations and consultancy projects with industry and academic institutions in the UK, Italy, Hungary, Libya, Malaysia, Thailand, Iraq and Saudi Arabia. He has published over 230 technical papers and has delivered more than 60 invited keynotes/lectures/seminars/short courses around the world. He has supervised 24 PhD students to completion and is currently supervising 10 PhD students. He is the author of 'Batch Distillation: Design & Operation' (text book) published by the Imperial College Press, London, 2004 which is based on his 18 years of research in Batch Distillation.

APPENDIX

Table A

Weights, bias and transfer function of neural network (20 neurons) (1st ANN model)

Weights 1 st layer	Weight size for 1 st layer [20x3]				Bias size [20x1]		Transfer function
$w_{1,1}^1 =$	-2.340	$w_{21}^1 =$	7.202	$w_{3,1}^1 =$	8.285	B_1^1	$f_1^1 = \tanh$
$w_{1,2}^1 =$	3.119	$w_{2,2}^1 =$	6.517	$w_{3,2}^1 =$	-1.800	B_2^1	$f_2^1 = \tanh$
$w_{1,3}^1 =$	-0.109	$w_{2,3}^1 =$	1.819	$w_{3,3}^1 =$	-5.171	B_3^1	$f_3^1 = \tanh$
$w_{1,4}^1 =$	0.091	$w_{2,4}^1 =$	-2.655	$w_{3,4}^1 =$	3.740	B_4^1	$f_4^1 = \tanh$
$w_{1,5}^1 =$	1.240	$w_{2,5}^1 =$	0.462	$w_{3,5}^1 =$	-0.086	B_5^1	$f_5^1 = \tanh$
$w_{1,6}^1 =$	7.711	$w_{2,6}^1 =$	-4.299	$w_{3,6}^1 =$	9.855	B_6^1	$f_6^1 = \tanh$
$w_{1,7}^1 =$	4.056	$w_{2,7}^1 =$	-2.964	$w_{3,7}^1 =$	-4.874	B_7^1	$f_7^1 = \tanh$
$w_{1,8}^1 =$	1.124	$w_{2,8}^1 =$	1.893	$w_{3,8}^1 =$	0.971	B_8^1	$f_8^1 = \tanh$
$w_{1,9}^1 =$	-0.058	$w_{2,9}^1 =$	2.534	$w_{3,9}^1 =$	-1.215	B_9^1	$f_9^1 = \tanh$
$w_{1,10}^1 =$	-4.128	$w_{2,10}^1 =$	-0.295	$w_{3,10}^1 =$	-0.149	B_{10}^1	$f_{10}^1 = \tanh$
$w_{1,11}^1 =$	-6.671	$w_{2,11}^1 =$	2.649	$w_{3,11}^1 =$	-5.390	B_{11}^1	$f_{11}^1 = \tanh$
$w_{1,12}^1 =$	0.022	$w_{2,12}^1 =$	0.867	$w_{3,12}^1 =$	-3.115	B_{12}^1	$f_{12}^1 = \tanh$
$w_{1,13}^1 =$	-0.061	$w_{2,13}^1 =$	2.029	$w_{3,13}^1 =$	0.009	B_{13}^1	$f_{13}^1 = \tanh$
$w_{1,14}^1 =$	-3.183	$w_{2,14}^1 =$	-8.906	$w_{3,14}^1 =$	-1.264	B_{14}^1	$f_{14}^1 = \tanh$
$w_{1,15}^1 =$	3.911	$w_{2,15}^1 =$	-1.955	$w_{3,15}^1 =$	-4.045	B_{15}^1	$f_{15}^1 = \tanh$
$w_{1,16}^1 =$	-0.055	$w_{2,16}^1 =$	0.330	$w_{3,16}^1 =$	-0.629	B_{16}^1	$f_{16}^1 = \tanh$
$w_{1,17}^1 =$	0.003	$w_{2,17}^1 =$	-0.644	$w_{3,17}^1 =$	-1.888	B_{17}^1	$f_{17}^1 = \tanh$
$w_{1,18}^1 =$	3.208	$w_{2,18}^1 =$	1.796	$w_{3,18}^1 =$	-2.444	B_{18}^1	$f_{18}^1 = \tanh$
$w_{1,19}^1 =$	-0.087	$w_{2,19}^1 =$	3.662	$w_{3,19}^1 =$	-1.591	B_{19}^1	$f_{19}^1 = \tanh$
$w_{1,20}^1 =$	0.126	$w_{2,20}^1 =$	1.734	$w_{3,20}^1 =$	1.405	B_{20}^1	$f_{20}^1 = \tanh$
Weight 2 nd layer	Weight size for 2 nd layer [20x3]				Bias size [3x1]		Transfer function
$w_{1,1}^2 =$	0.070	$w_{1,2}^2 =$	0.040	$w_{1,3}^2 =$	0.008	B_1^2	$f_1^3 = 1$
$w_{2,1}^2 =$	0.027	$w_{2,2}^2 =$	0.017	$w_{2,3}^2 =$	0.012	B_2^2	
$w_{3,1}^2 =$	0.347	$w_{3,2}^2 =$	0.417	$w_{3,3}^2 =$	0.347	B_3^3	
$w_{4,1}^2 =$	0.761	$w_{4,2}^2 =$	0.849	$w_{4,3}^2 =$	0.744		
$w_{5,1}^2 =$	0.039	$w_{5,2}^2 =$	0.039	$w_{5,3}^2 =$	0.042		
$w_{6,1}^2 =$	-0.003	$w_{6,2}^2 =$	-0.007	$w_{6,3}^2 =$	-0.035		
$w_{7,1}^2 =$	-0.037	$w_{7,2}^2 =$	-0.039	$w_{7,3}^2 =$	-0.048		
$w_{8,1}^2 =$	-0.042	$w_{8,2}^2 =$	-0.017	$w_{8,3}^2 =$	0.025		
$w_{9,1}^2 =$	-2.309	$w_{9,2}^2 =$	-2.383	$w_{9,3}^2 =$	-1.982		
$w_{10,1}^2 =$	0.030	$w_{10,2}^2 =$	0.041	$w_{10,3}^2 =$	0.043		
$w_{11,1}^2 =$	0.006	$w_{11,2}^2 =$	-0.002	$w_{11,3}^2 =$	-0.021		
$w_{12,1}^2 =$	0.198	$w_{12,2}^2 =$	0.191	$w_{12,3}^2 =$	0.153		
$w_{13,1}^2 =$	0.399	$w_{13,2}^2 =$	0.410	$w_{13,3}^2 =$	0.197		
$w_{14,1}^2 =$	-0.045	$w_{14,2}^2 =$	-0.038	$w_{14,3}^2 =$	-0.006		
$w_{15,1}^2 =$	0.028	$w_{15,2}^2 =$	0.031	$w_{15,3}^2 =$	0.030		
$w_{16,1}^2 =$	-0.692	$w_{16,2}^2 =$	-0.467	$w_{16,3}^2 =$	0.755		
$w_{17,1}^2 =$	-0.780	$w_{17,2}^2 =$	-0.767	$w_{17,3}^2 =$	-0.816		
$w_{18,1}^2 =$	0.041	$w_{18,2}^2 =$	0.041	$w_{18,3}^2 =$	0.046		
$w_{19,1}^2 =$	1.296	$w_{19,2}^2 =$	1.350	$w_{19,3}^2 =$	0.922		
$w_{20,1}^2 =$	-0.424	$w_{20,2}^2 =$	-0.457	$w_{20,3}^2 =$	-0.373		

Table B

Weights, bias and transfer function of neural network (20 neurons) (2nd ANN model)*.

Weights 1 st layer	Weight size for 1 st layer [20x2]			Bias	size [20x1]	Transfer function		
$w_{1,1}^1 =$	3.641	$w_{2,1}^1 =$	4.651	B_1^1	-6.061	$f_1^1 = \tanh$		
$w_{1,2}^1 =$	-3.367	$w_{2,2}^1 =$	6.123	B_2^1	5.411	$f_2^1 = \tanh$		
$w_{1,3}^1 =$	-2.667	$w_{2,3}^1 =$	5.405	B_3^1	4.263	$f_3^1 = \tanh$		
$w_{1,4}^1 =$	-2.598	$w_{2,4}^1 =$	-5.587	B_4^1	3.939	$f_4^1 = \tanh$		
$w_{1,5}^1 =$	5.967	$w_{2,5}^1 =$	-1.332	B_5^1	-3.678	$f_5^1 = \tanh$		
$w_{1,6}^1 =$	-3.770	$w_{2,6}^1 =$	-5.178	B_6^1	3.533	$f_6^1 = \tanh$		
$w_{1,7}^1 =$	8.412	$w_{2,7}^1 =$	-3.426	B_7^1	-2.545	$f_7^1 = \tanh$		
$w_{1,8}^1 =$	-3.650	$w_{2,8}^1 =$	-6.020	B_8^1	1.169	$f_8^1 = \tanh$		
$w_{1,9}^1 =$	0.532	$w_{2,9}^1 =$	-6.467	B_9^1	0.997	$f_9^1 = \tanh$		
$w_{1,10}^1 =$	5.699	$w_{2,10}^1 =$	1.136	B_{10}^1	-1.574	$f_{10}^1 = \tanh$		
$w_{1,11}^1 =$	3.181	$w_{2,11}^1 =$	4.802	B_{11}^1	1.013	$f_{11}^1 = \tanh$		
$w_{1,12}^1 =$	-7.066	$w_{2,12}^1 =$	-0.221	B_{12}^1	-0.206	$f_{12}^1 = \tanh$		
$w_{1,13}^1 =$	6.416	$w_{2,13}^1 =$	0.618	B_{13}^1	0.412	$f_{13}^1 = \tanh$		
$w_{1,14}^1 =$	-5.754	$w_{2,14}^1 =$	3.587	B_{14}^1	-3.039	$f_{14}^1 = \tanh$		
$w_{1,15}^1 =$	4.747	$w_{2,15}^1 =$	2.643	B_{15}^1	3.083	$f_{15}^1 = \tanh$		
$w_{1,16}^1 =$	5.735	$w_{2,16}^1 =$	-0.069	B_{16}^1	4.800	$f_{16}^1 = \tanh$		
$w_{1,17}^1 =$	-0.280	$w_{2,17}^1 =$	6.017	B_{17}^1	5.153	$f_{17}^1 = \tanh$		
$w_{1,18}^1 =$	1.990	$w_{2,18}^1 =$	-5.681	B_{18}^1	4.090	$f_{18}^1 = \tanh$		
$w_{1,19}^1 =$	3.572	$w_{2,19}^1 =$	2.182	B_{19}^1	5.249	$f_{19}^1 = \tanh$		
$w_{1,20}^1 =$	-5.481	$w_{2,20}^1 =$	-2.805	B_{20}^1	-7.229	$f_{20}^1 = \tanh$		
Weight 2 nd layer	Weight size for 2 nd layer [20x3]				Bias	size [3x1]	Transfer function	
$w_{1,1}^2 =$	0.056	$w_{1,2}^2 =$	0.038	$w_{1,3}^2 =$	-0.008	B_1^2	0.050	$f_1^3 = 1$
$w_{2,1}^2 =$	-0.702	$w_{2,2}^2 =$	-0.482	$w_{2,3}^2 =$	-0.703	B_2^2	0.018	
$w_{3,1}^2 =$	0.900	$w_{3,2}^2 =$	0.651	$w_{3,3}^2 =$	0.725	B_3^3	0.075	
$w_{4,1}^2 =$	-0.034	$w_{4,2}^2 =$	-0.001	$w_{4,3}^2 =$	-0.018			
$w_{5,1}^2 =$	-0.610	$w_{5,2}^2 =$	-0.660	$w_{5,3}^2 =$	-0.409			
$w_{6,1}^2 =$	0.110	$w_{6,2}^2 =$	0.062	$w_{6,3}^2 =$	0.012			
$w_{7,1}^2 =$	-0.050	$w_{7,2}^2 =$	-0.030	$w_{7,3}^2 =$	-0.227			
$w_{8,1}^2 =$	0.012	$w_{8,2}^2 =$	0.004	$w_{8,3}^2 =$	0.000			
$w_{9,1}^2 =$	0.000	$w_{9,2}^2 =$	0.013	$w_{9,3}^2 =$	0.007			
$w_{10,1}^2 =$	-0.255	$w_{10,2}^2 =$	0.015	$w_{10,3}^2 =$	-0.133			
$w_{11,1}^2 =$	-0.027	$w_{11,2}^2 =$	0.011	$w_{11,3}^2 =$	0.040			
$w_{12,1}^2 =$	-1.343	$w_{12,2}^2 =$	0.294	$w_{12,3}^2 =$	0.330			
$w_{13,1}^2 =$	-1.132	$w_{13,2}^2 =$	0.180	$w_{13,3}^2 =$	0.155			
$w_{14,1}^2 =$	0.061	$w_{14,2}^2 =$	0.020	$w_{14,3}^2 =$	0.020			
$w_{15,1}^2 =$	-0.019	$w_{15,2}^2 =$	-0.020	$w_{15,3}^2 =$	-0.058			
$w_{16,1}^2 =$	0.027	$w_{16,2}^2 =$	0.027	$w_{16,3}^2 =$	-0.023			
$w_{17,1}^2 =$	0.071	$w_{17,2}^2 =$	0.025	$w_{17,3}^2 =$	-0.020			
$w_{18,1}^2 =$	-0.015	$w_{18,2}^2 =$	-0.002	$w_{18,3}^2 =$	0.008			
$w_{19,1}^2 =$	0.775	$w_{19,2}^2 =$	0.382	$w_{19,3}^2 =$	1.184			
$w_{20,1}^2 =$	0.850	$w_{20,2}^2 =$	0.437	$w_{20,3}^2 =$	1.191			

*without considering feed flow rate

Table C
Data used in the 1st ANN Model

No.	F (kg/hr)	T (°C)	P (kPa)	Y ₁	Y ₂	Y ₃	No.	F (kg/hr)	T (°C)	P (kPa)	Y ₁	Y ₂	Y ₃
1	1000	100	0.00000	0.00052	0.00088	0.98	71	1500	125	0.00040	0.00056	0.00091	0.99
2	1000	100	0.00010	0.00056	0.00091	1.00	72	1500	125	0.00050	0.00056	0.00091	0.99
3	1000	100	0.00020	0.00056	0.00091	1.00	73	1500	125	0.00060	0.00056	0.00091	0.99
4	1000	100	0.00030	0.00056	0.00090	1.00	74	1500	125	0.00070	0.00056	0.00091	1.00
5	1000	100	0.00040	0.00056	0.00090	1.00	75	1500	125	0.00080	0.00056	0.00091	1.00
6	1000	100	0.00050	0.00056	0.00090	1.00	76	1500	125	0.00090	0.00056	0.00091	1.00
7	1000	100	0.00060	0.00055	0.00089	1.00	77	1500	125	0.00100	0.00056	0.00091	1.00
8	1000	100	0.00070	0.00055	0.00089	1.00	78	1500	150	0.00000	0.00003	0.00005	0.09
9	1000	100	0.00080	0.00055	0.00089	1.00	79	1500	150	0.00010	0.00038	0.00067	0.65
10	1000	100	0.00090	0.00055	0.00089	1.00	80	1500	150	0.00020	0.00047	0.00078	0.80
11	1000	100	0.00100	0.00055	0.00089	1.00	81	1500	150	0.00030	0.00050	0.00083	0.86
12	1000	125	0.00000	0.00031	0.00062	0.73	82	1500	150	0.00040	0.00052	0.00085	0.89
13	1000	125	0.00010	0.00053	0.00088	0.97	83	1500	150	0.00050	0.00053	0.00086	0.91
14	1000	125	0.00020	0.00055	0.00090	0.98	84	1500	150	0.00060	0.00053	0.00087	0.93
15	1000	125	0.00030	0.00056	0.00090	0.99	85	1500	150	0.00070	0.00054	0.00088	0.94
16	1000	125	0.00040	0.00056	0.00091	0.99	86	1500	150	0.00080	0.00054	0.00088	0.95
17	1000	125	0.00050	0.00056	0.00091	0.99	87	1500	150	0.00090	0.00055	0.00089	0.95
18	1000	125	0.00060	0.00056	0.00091	0.99	88	1500	150	0.00100	0.00055	0.00089	0.96
19	1000	125	0.00070	0.00056	0.00091	1.00	89	1500	175	0.00000	0.00000	0.00001	0.07
20	1000	125	0.00080	0.00056	0.00091	1.00	90	1500	175	0.00010	0.00000	0.00001	0.07
21	1000	125	0.00090	0.00056	0.00091	1.00	91	1500	175	0.00020	0.00017	0.00027	0.18
22	1000	125	0.00100	0.00056	0.00091	1.00	92	1500	175	0.00030	0.00027	0.00043	0.29
23	1000	150	0.00000	0.00003	0.00005	0.09	93	1500	175	0.00040	0.00033	0.00054	0.38
24	1000	150	0.00010	0.00038	0.00067	0.65	94	1500	175	0.00050	0.00038	0.00061	0.46
25	1000	150	0.00020	0.00047	0.00078	0.80	95	1500	175	0.00060	0.00041	0.00065	0.52
26	1000	150	0.00030	0.00050	0.00083	0.86	96	1500	175	0.00070	0.00043	0.00069	0.56
27	1000	150	0.00040	0.00052	0.00085	0.89	97	1500	175	0.00080	0.00045	0.00072	0.60
28	1000	150	0.00050	0.00053	0.00086	0.91	98	1500	175	0.00090	0.00046	0.00074	0.64
29	1000	150	0.00060	0.00053	0.00087	0.93	99	1500	175	0.00100	0.00047	0.00076	0.66
30	1000	150	0.00070	0.00054	0.00088	0.94	100	1500	200	0.00000	0.00000	0.00000	0.06
31	1000	150	0.00080	0.00054	0.00088	0.95	101	1500	200	0.00010	0.00001	0.00002	0.07
32	1000	150	0.00090	0.00055	0.00089	0.95	102	1500	200	0.00020	0.00003	0.00003	0.07
33	1000	150	0.00100	0.00055	0.00089	0.96	103	1500	200	0.00030	0.00004	0.00005	0.08
34	1000	175	0.00000	0.00000	0.00001	0.07	104	1500	200	0.00040	0.00006	0.00007	0.08
35	1000	175	0.00010	0.00000	0.00001	0.07	105	1500	200	0.00050	0.00007	0.00010	0.08
36	1000	175	0.00020	0.00017	0.00027	0.18	106	1500	200	0.00060	0.00009	0.00012	0.09
37	1000	175	0.00030	0.00027	0.00043	0.29	107	1500	200	0.00070	0.00011	0.00014	0.10
38	1000	175	0.00040	0.00033	0.00054	0.38	108	1500	200	0.00080	0.00013	0.00017	0.10
39	1000	175	0.00050	0.00038	0.00061	0.46	109	1500	200	0.00090	0.00015	0.00020	0.11
40	1000	175	0.00060	0.00041	0.00065	0.52	110	1500	200	0.00100	0.00017	0.00023	0.12
41	1000	175	0.00070	0.00043	0.00069	0.56	111	2000	100	0.00000	0.00052	0.00088	0.98
42	1000	175	0.00080	0.00045	0.00072	0.60	112	2000	100	0.00010	0.00056	0.00091	1.00
43	1000	175	0.00090	0.00046	0.00074	0.64	113	2000	100	0.00020	0.00056	0.00091	1.00
44	1000	175	0.00100	0.00047	0.00076	0.66	114	2000	100	0.00030	0.00056	0.00090	1.00
45	1000	200	0.00000	0.00000	0.00000	0.06	115	2000	100	0.00040	0.00056	0.00090	1.00
46	1000	200	0.00010	0.00001	0.00002	0.07	116	2000	100	0.00050	0.00056	0.00090	1.00
47	1000	200	0.00020	0.00003	0.00003	0.07	117	2000	100	0.00060	0.00055	0.00089	1.00
48	1000	200	0.00030	0.00004	0.00005	0.08	118	2000	100	0.00070	0.00055	0.00089	1.00
49	1000	200	0.00040	0.00006	0.00007	0.08	119	2000	100	0.00080	0.00055	0.00089	1.00
50	1000	200	0.00050	0.00007	0.00010	0.08	120	2000	100	0.00090	0.00055	0.00089	1.00
51	1000	200	0.00060	0.00009	0.00012	0.09	121	2000	100	0.00100	0.00055	0.00089	1.00
52	1000	200	0.00070	0.00011	0.00014	0.10	122	2000	125	0.00000	0.00031	0.00062	0.73
53	1000	200	0.00080	0.00013	0.00017	0.10	123	2000	125	0.00010	0.00053	0.00088	0.97
54	1000	200	0.00090	0.00015	0.00020	0.11	124	2000	125	0.00020	0.00055	0.00090	0.98
55	1000	200	0.00100	0.00017	0.00023	0.12	125	2000	125	0.00030	0.00056	0.00090	0.99
56	1500	100	0.00000	0.00052	0.00088	0.98	126	2000	125	0.00040	0.00056	0.00091	0.99
57	1500	100	0.00010	0.00056	0.00091	1.00	127	2000	125	0.00050	0.00056	0.00091	0.99
58	1500	100	0.00020	0.00056	0.00091	1.00	128	2000	125	0.00060	0.00056	0.00091	0.99
59	1500	100	0.00030	0.00056	0.00090	1.00	129	2000	125	0.00070	0.00056	0.00091	1.00
60	1500	100	0.00040	0.00056	0.00090	1.00	130	2000	125	0.00080	0.00056	0.00091	1.00
61	1500	100	0.00050	0.00056	0.00090	1.00	131	2000	125	0.00090	0.00056	0.00091	1.00
62	1500	100	0.00060	0.00055	0.00089	1.00	132	2000	125	0.00100	0.00056	0.00091	1.00
63	1500	100	0.00070	0.00055	0.00089	1.00	133	2000	150	0.00000	0.00003	0.00005	0.09
64	1500	100	0.00080	0.00055	0.00089	1.00	134	2000	150	0.00010	0.00038	0.00067	0.65
65	1500	100	0.00090	0.00055	0.00089	1.00	135	2000	150	0.00020	0.00047	0.00078	0.80
66	1500	100	0.00100	0.00055	0.00089	1.00	136	2000	150	0.00030	0.00050	0.00083	0.86
67	1500	125	0.00000	0.00031	0.00062	0.73	137	2000	150	0.00040	0.00052	0.00085	0.89
68	1500	125	0.00010	0.00053	0.00088	0.97	138	2000	150	0.00050	0.00053	0.00086	0.91
69	1500	125	0.00020	0.00055	0.00090	0.98	139	2000	150	0.00060	0.00053	0.00087	0.93
70	1500	125	0.00030	0.00056	0.00090	0.99	140	2000	150	0.00070	0.00054	0.00088	0.94

Table 1 cont'd

No.	F (kg/hr)	T (°C)	P (kPa)	Y ₁	Y ₂	Y ₃	No.	F (kg/hr)	T (°C)	P (kPa)	Y ₁	Y ₂	Y ₃
141	<i>2000</i>	<i>150</i>	<i>0.00080</i>	<i>0.00054</i>	<i>0.00088</i>	<i>0.95</i>	154	2000	175	0.00100	0.00046	0.00074	0.64
142	2000	150	0.00090	0.00055	0.00089	0.95	155	2000	200	0.00000	0.00047	0.00076	0.66
143	2000	150	0.00100	0.00055	0.00089	0.96	156	2000	200	0.00010	0.00000	0.00000	0.06
144	2000	175	0.00000	0.00000	0.00001	0.07	157	2000	200	0.00020	0.00001	0.00002	0.07
145	2000	175	0.00010	0.00000	0.00001	0.07	158	2000	200	0.00030	0.00003	0.00003	0.07
146	2000	175	0.00020	0.00017	0.00027	0.18	159	2000	200	0.00040	0.00004	0.00005	0.08
147	2000	175	0.00030	0.00027	0.00043	0.29	160	2000	200	0.00050	0.00006	0.00007	0.08
148	2000	175	0.00040	0.00033	0.00054	0.38	161	2000	200	0.00060	0.00007	0.00010	0.08
149	2000	175	0.00050	0.00038	0.00061	0.46	162	<i>2000</i>	<i>200</i>	<i>0.00070</i>	<i>0.00009</i>	<i>0.00012</i>	<i>0.09</i>
150	2000	175	0.00060	0.00041	0.00065	0.52	163	<i>2000</i>	<i>200</i>	<i>0.00080</i>	<i>0.00011</i>	<i>0.00014</i>	<i>0.10</i>
151	<i>2000</i>	<i>175</i>	<i>0.00070</i>	<i>0.00043</i>	<i>0.00069</i>	<i>0.56</i>	164	2000	200	0.00090	0.00013	0.00017	0.10
152	<i>2000</i>	<i>175</i>	<i>0.00080</i>	<i>0.00045</i>	<i>0.00072</i>	<i>0.60</i>	165	2000	200	0.00100	0.00015	0.00020	0.11
153	2000	175	0.00090	0.00054	0.00088	0.95							

Note: Bold data for Training, Italic data for Validation, Plain data in Test.